Catalysis Letters 36 (1996) 59–68

n-butane isomerization on sulfated zirconia. Deactivation and regeneration as studied by Raman, UV-VIS diffuse reflectance and ESR spectroscopy

D. Spielbauer, G.A.H. Mekhemer [1], E. Bosch and H. Knözinger [2]

Institut für Physikalische Chemie, Universität München, Sophienstrasse 11, 80333 Munich, Germany

Received 13 June 1995; accepted 3 October 1995

n-butane isomerization on sulfated zirconia was studied in the temperature range 393–473 K. Rapid deactivation occurs, when the reaction is carried out in He carrier gas. In contrast, stable stationary activity was observed in H_2 carrier gas. In situ Raman and UV-VIS diffuse reflectance spectroscopy and ESR showed that the deactivation is caused by the formation of allylic and polyenylic cations and polycyclic aromatic compounds, the formation of which is largely prevented in the presence of H_2. Deactivated catalysts can be fully regenerated by treatment at 723–753 K in flowing O_2. The regeneration process was also followed by in situ spectroscopies.

Keywords: zirconia-sulfated; *n*-butane; isomerization; deactivation; regeneration; Raman spectroscopy; UV-VIS diffuse reflectance; ESR

1. Introduction

Sulfated metal oxides such as ZrO_2 [1] and TiO_2 [2,3] have been claimed to develop superacidity. Sulfated ZrO_2 has in fact been shown to catalyze the skeletal isomerization of *n*-butane into isobutane [4,5]. Acid-catalyzed transformations of saturated hydrocarbons, such as fragmentation, alkylation, and isomerization, are generally considered to involve carbocation intermediates [6] that can be generated by the attack of the alkane molecule by acid sites via three different routes: (i) hydride abstraction by Lewis acid sites; (ii) the attack of a C–H bond by the proton of a Brønsted acid site; and (iii) the attack of a C–C bond by Brønsted acid sites (protolysis).

The isomerization of *n*-butane on so-called superacidic solids has been studied frequently because of the technological importance of isobutane for the alkylation of alkenes [7,8]. Also, *n*-butane is expected to convert at slow reaction rates and to yield a simple product distribution [9]. Recently, Adeeva et al. [10] have questioned the superacidic character of sulfated ZrO_2, and Adeeva et al. [11] have shown by ^{13}C-labelling experiments that the transformation of *n*-butane is a bimolecular process with octane intermediates.

Dimeric species might also be intermediates that can lead to coke. As a matter of fact, the *n*-butane isomerization on sulfated ZrO_2 always suffers from severe deactivation with time-on-stream within very short initial time periods. It has been shown, that the use of a Pt-containing sulfated ZrO_2 catalyst [12] and/or the addition of hydrogen to the reaction feed [9,13] prevents or strongly reduces the deactivation. It has been proposed that hydrogen may retard the reaction by either inhibiting the dehydrogenation step that leads to the formation of carbenium ions or by blocking of active sites.

The nature of the coke that is deposited onto the catalyst surface during *n*-butane isomerization on sulfated ZrO_2 is still unknown. Also, the chemistry occurring during regeneration procedures has not been studied. The aim of the present paper therefore is to (i) characterize the coke deposits formed on sufated ZrO_2 during *n*-butane isomerization in the absence of hydrogen, (ii) study the effect of hydrogen in the reaction mixture on the coke formation; and (iii) follow the chemistry occurring during oxidative regeneration processes. The characterization of the catalysts and of coke deposits was carried out by means of in situ laser Raman, by UV-VIS diffuse reflectance spectroscopy and by electron spin resonance.

2. Experimental

Sulfated zirconium hydroxide type XZO 682/1 from MEL Chemicals, Manchester, UK was calcined in static air at 873 K for 1 h to produce sulfated ZrO_2, henceforth denoted ZrO_2/SO_4. The BET surface area of this material was 100 m^2/g. XRD indicated a mixture of the tetragonal (t-ZrO_2) and the monoclinic (m-ZrO_2) phase (75/25). For in situ activation prior to starting the catalytic conversion of *n*-butane, the catalyst material was heated

[1] Present address: Department of Chemistry, Minia University, El Minia, Egypt.

[2] To whom correspondence should be addressed.

at 723–753 K for 1 h in a flow of hydrocarbon-free dry oxygen (Linde AG, $\geqslant$ 99.6%). The regeneration of the deactivated catalysts was performed under identical conditions. In some experiments, however, water vapour (23 mbar) was added to the O_2 flow.

Catalytic conversions were carried out at atmospheric pressure in a fixed bed quartz flow reactor. 1 g of catalyst powder was placed between quartz wool plugs. *n*-butane (Linde AG, $\geqslant$ 99.5%) at constant partial pressure was introduced at a flow rate of 3 ml/min into the carrier gas flow of either helium (35 ml/min, Linde AG, $\geqslant$99.996%) or hydrogen (40 ml/min, Linde AG, $\geqslant$99.999%) at preselected bed temperatures. The *n*-butane partial pressures were 85 mbar in He and 75 mbar in H_2. The product analyses were carried out by gas chromatography on a PoraPLOT Q capillary column using a Varian model 3400 chromatograph equipped with a flame ionization detector.

For laser Raman spectroscopy (LRS) an in situ Raman cell that was described previously [14], was used. This cell allowed the heating of the samples at temperatures up to 770 K in the presence of either static or flowing gas atmospheres of any kind. The spectra can be recorded under catalytic conditions. Catalyst samples were pressed into special stainless steel holders. Raman spectra were recorded on a Dilor (OMARS 89) spectrometer which was equipped with a Princeton Applied Instruments optical multichannel analyzer (OMA). The Raman spectra were excited by the 488 nm line of an Ar^+-ion laser model series 2020 from Spectra Physics. For the catalytic in situ experiments in a *n*-butane/He flow the laser power at the sample position was limited to 3 mW. All other spectra were recorded at 30 mW laser power. Spectra were recorded using the scanning multichannel technique (SMT) [15].

Samples for UV-VIS diffuse reflectance spectroscopy (DRS) and ESR were prepared in a U-tube reactor under conditions that were identical to those of the catalytic conversion measurements. The reactor was connected to an ESR-tube and to a UV-VIS quartz cell. The whole system could be tightly closed and removed from the vacuum and gas line. By turning the U-tube reactor, the catalyst powder could be filled into either the ESR-tube or the optical cell without exposure to any uncontrolled atmosphere.

A Perkin-Elmer Lambda 15 spectrometer with a $BaSO_4$-coated integrating sphere was used for DRS, the data being transferred to a PC for further treatment. Spectra were recorded at room temperature using $BaSO_4$ as a reference material. The DR spectra are plotted as absorbance $(1 - R_\infty)$ vs. wavelength, where R_∞ is the reflectance relative to the $BaSO_4$ reference for a sample of infinite thickness (layer thickness in quartz cell: 5 mm).

ESR measurements were carried out on a Varian E-Line (E 9) spectrometer which was equipped with a TE_{104}-mode double cavity. All spectra were recorded in the X-band at room temperature with a microwave power of 10 mW, and the data were transferred to a PC for further treatment [16]. A Mn^{2+} solid solution in MgO was used as a reference material. Samples that were treated in O_2 or H_2O/O_2 were repeatedly evacuated to < 10 mbar at room temperatur and exposed to helium.

3. Results and discussion

3.1. Catalytic n-butane conversion

The activated ZrO_2/SO_4 was active for *n*-butane isomerization and product distributions were measured in the temperature range 393–473 K as a function of time-on-stream under the conditions specified above. As shown in fig. 1A the initial conversion (measured after 1 min on-stream) in a He flow at 453 K was 38% for a freshly activated catalyst and decayed within approximately 100 min to an almost stationary conversion of 12%. After 360 min on-stream, this deactivated catalyst was regenerated in a flow of dry O_2. Thereafter, the catalytic behaviour was fully restored as shown in fig. 1A.

At temperatures $\leqslant$423 K isobutane was the only detectable product and it remained the dominant product in the entire temperature range up to 473 K. At temperatures $\geqslant$423 K additional products, particularly propane and *n*-pentane were also formed in small quantities consistent with the intermediate formation of *n*-octane [11]. As an example, fig. 1B shows the product distribution as a function of time-on-stream that was observed at 473 K in He carrier gas. There is a remarkable formation of propane during the initial reaction period while the amounts of both by-products remained below 2% in the steady-state regime after the initial deactivation period.

Fig. 2A shows the conversion as a function of time-on-stream that was obtained when the reaction was carried out at 473 K in a H_2 flow. In contrast to the reaction in He flow (fig. 1A) where deactivation started immediately after introduction of the *n*-butane feed, an induction period of approximately 100 min is observed in H_2 flow in which time period the conversion increased from an initial value of 19–20% to a steady-state value of 27%. As shown in the product distribution (fig. 2B), clearly isobutane is the dominant product also in H_2 flow, although the amount of propane formed is somewhat higher than in He flow under steady-state conditions, and small amounts of additional products, namely methane, ethane and *n*-pentane are also observed. The selectivity to isobutane, however, is only slightly reduced in H_2 as compared to He. It should also be noted that the steady-state conversion of *n*-butane in H_2 was more than twice that in He despite the slightly higher H_2 flow rate.

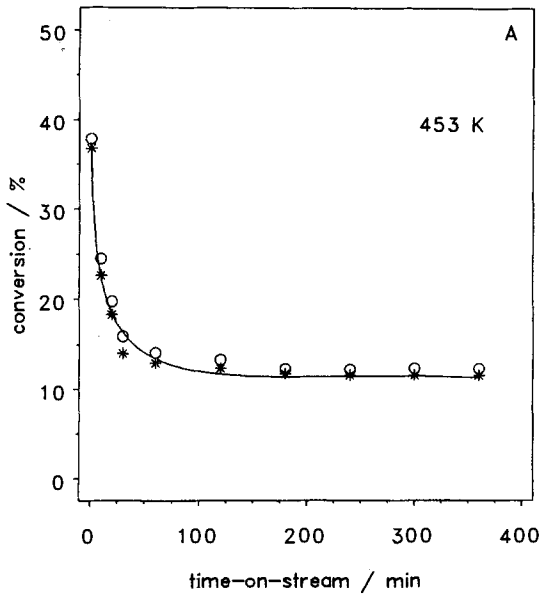

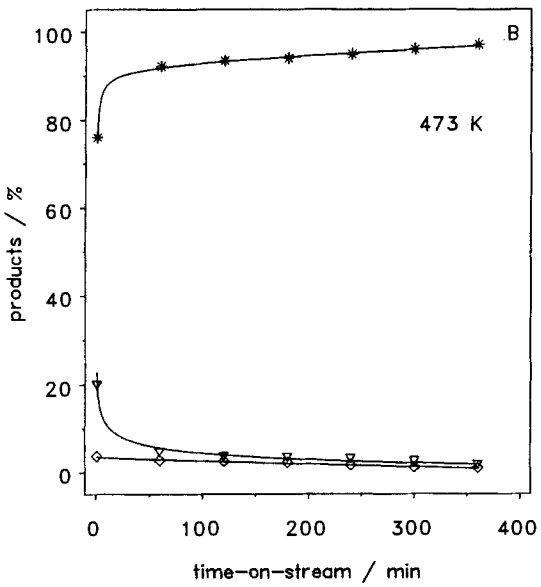

Fig. 1. (A) *n*-butane conversion in He flow on the (○) fresh and (*) regenerated ZrO_2/SO_4 at 453 K; (B) product distribution of the *n*-butane isomerization on ZrO_2/SO_4, in He at 473 K; (*) isobutane, (▽) propane, (◇) *n*-pentane.

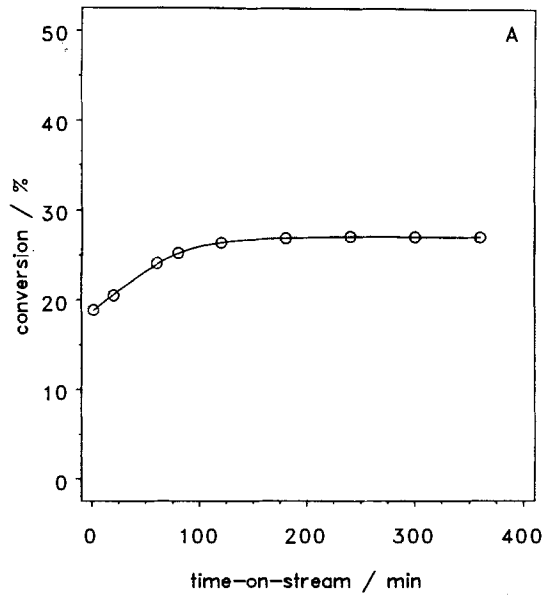

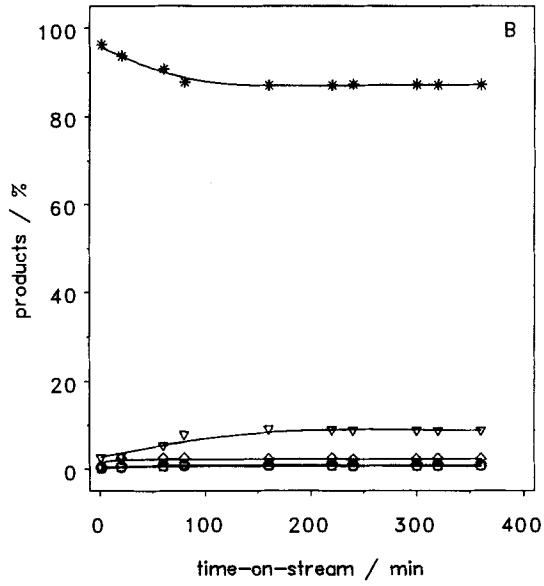

Fig. 2. (A) *n*-butane conversion in H_2 flow on ZrO_2/SO_4 at 473 K; (B) product distribution of the *n*-butane isomerization on ZrO_2/SO_4 in H_2 at 473 K; (*) isobutane, (▽) propane, (◇) *n*-pentane, (○) ethane, (□) methane.

3.2. Raman spectroscopy

The Raman spectrum of the activated sample (spectrum a in fig. 3) shows several bands in the wavenumber range below 800 cm^{-1} which can be assigned to Zr–O vibrations. Bands at 150 and 274 cm^{-1} are indicative for t-ZrO_2, bands at 188, 330 and 375 cm^{-1} are indicative for m-ZrO_2. The bands at 1000 and 1031 cm^{-1}, and at 1400 cm^{-1} are to be attributed to S–O and S=O stretching modes of the sulfate group, respectively. As reported earlier [17], the surface sulfate has a triply bridging structure with C_s symmetry.

Spectrum b in fig. 3 was recorded in situ after the sample had been exposed to *n*-butane/He at 473 K for 1 h. The sample showed a high background, which is caused by fluorescence and recommends a baseline subtraction. This fluorescence probably originates from a broad absorption band of the ZrO_2/SO_4 catalyst after exposure to He/*n*-butane at 473 K which is located at 400 nm (spectrum a in fig. 5). Comparing this Raman spectrum with the baseline subtracted spectrum of the activated sample, most of the Zr–O signals can be identified. Additional new bands of organic contaminants are seen at (i) 300 (s, br) cm^{-1} (deformation vibrations of aliphatic C–C–C groups and bending vibrations of CC_3 groups), (ii) 725 (w) cm^{-1} (deformation vibrations of aromatic C–H

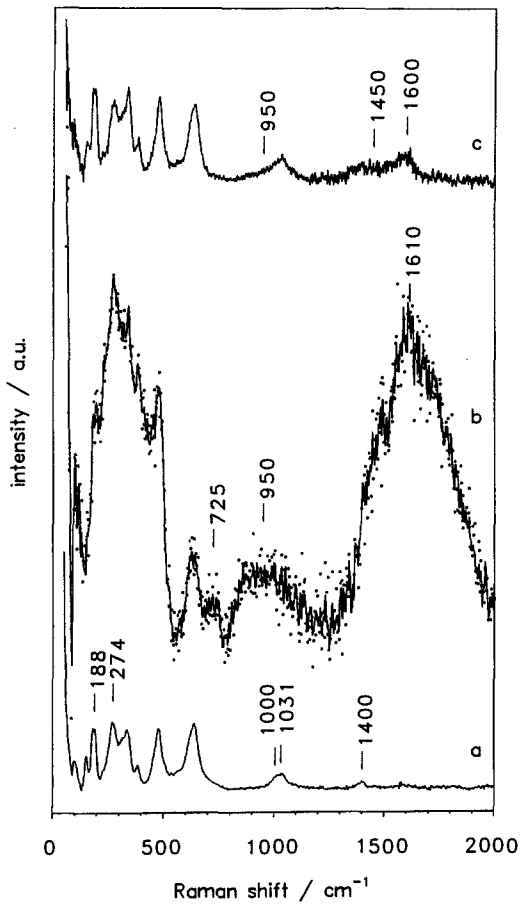

Fig. 3. In situ Raman spectra (baseline subtracted) of sulfated zirconia recorded at 473 K (a) activated sample; (b) after exposure to with He/*n*-butane for 1 h; (c) after exposure to flowing H_2/*n*-butane for 2 h.

groups and stretching vibrations of CC_3 groups), (iii) 950 (m, br) cm^{-1} (deformation vibrations of olefinic C–H groups), and (iv) 1610 (s, br) cm^{-1} (C=C stretching vibrations of olefins and aromatics) [18]. The position of this band is typical for C=C stretching vibrations of olefinic compounds. Lange et al. [8] reported a broad band at about 1600 cm^{-1} after adsorption of ethylene on H-mordenite, which they attributed to polyenic and/or aromatic products.

After 2 h on stream, the sample was cooled to room temperature in a He atmosphere and subsequently regenerated in a flow of dry oxygen at 753 K for 1 h. The Raman spectra of the fresh and the regenerated catalysts are identical as regards the positions and intensities of the bands as demonstrated for the sulfate bands in fig. 4A. This observation is consistent with the fact that the catalytic activity could be fully restored after regeneration (vide supra).

If the deactivated catalyst was treated in a flow of O_2/H_2O, the background of the Raman spectrum vanished already at room temperature after 2 h, and only weak bands at 300 and 1600 cm^{-1} of the organic deposits were identified (not shown).

The Raman spectrum of the catalyst after contact with a H_2/*n*-butane mixture at 473 K for 2 h shows only a moderate background. The baseline subtracted spectrum c in fig. 3 with additional bands at 950 (w, br), 1450 (w) and 1600 (m, br) cm^{-1} demonstrates the low deposition of organic contaminants. The small shift of the C=C stretching vibration from 1610 to 1600 cm^{-1} and the new band at 1450 cm^{-1} may be indicative for an increasing aromatic character of the products [20].

After 4 h in the reaction mixture, the sample was cooled to room temperature and regenerated in a flow of dry O_2 at 773 K for 1 h. Figs. 4B and 4C compare the Raman spectra of the fresh and the regenerated sample in the Zr–O and sulfate regions, respectively. These spectra clearly demonstrate that the catalyst structures remain unchanged during catalysis and regeneration under the conditions applied in the present study. It is particularly noteworthy that sulfate loss does not occur. We found significant sulfate loss by TGA/MS at temperatures $\geqslant$973 K only. Bensitel et al. [21] observed a beginning reduction of sulfate in an atmosphere of H_2 above 723 K measured by IR spectroscopy and TGA.

3.3. *UV-VIS-DR spectroscopy*

After contact of the catalyst with a He/*n*-butane mixture at 473 K for 90 min new bands are identified in the UV-VIS-DR spectrum at 245 (w), 306, 366, and 400 (br) nm (spectrum a in fig. 5). Chen et al. [22] reported a single absorption band at 292 nm in a similar experiment with ZrO_2/SO_4 and He/*n*-butane at 523 K, which they attributed to allylic cations. Following their arguments, the absorption band at 306 nm may be assigned to allylic cations. The absorption bands at 366 and 400 nm are characteristic of polyenylic cations of the type $[R_2C{=}CH{-}(CH{=}CH{-})_nCR_2]^+$ ($n = 1$; R = H, alkyl) [23,24] and aromatic compounds [23], respectively. From the mechanistic point of view, the formation of allylic and polyenylic cations may be induced in the presence of Lewis acidic centers (cus Zr^{4+}) by hydride abstraction [6].

For regeneration the catalyst was treated in a flow of dry O_2 from room temperature to 753 K analogous to the conditions used in the Raman experiment. After 30 min at room temperature no changes were observed (spectrum b in fig. 5). Treatment at 423 K for additional 30 min results in a minor broadening of the band at 366 nm and a moderate increase of the broad band at 400 nm (spectrum c in fig. 5). Above 423 K, the bands of the allylic and polyenylic cations vanished, and an intense broad absorption band with a maximum at approximately 415 nm appeared (spectra d and e in fig. 5), which could be assigned to polycyclic aromatic compounds and condensed rings [23]. At 723 K the broad absorption band starts to decrease (spectrum f in fig. 5) by oxidation of the organic contaminants. After a further treatment in a flow of dry oxygen at 753 K for 1 h the spectrum of the fresh catalyst was obtained. The weak absorption band at 245 nm is presumably caused by variations of

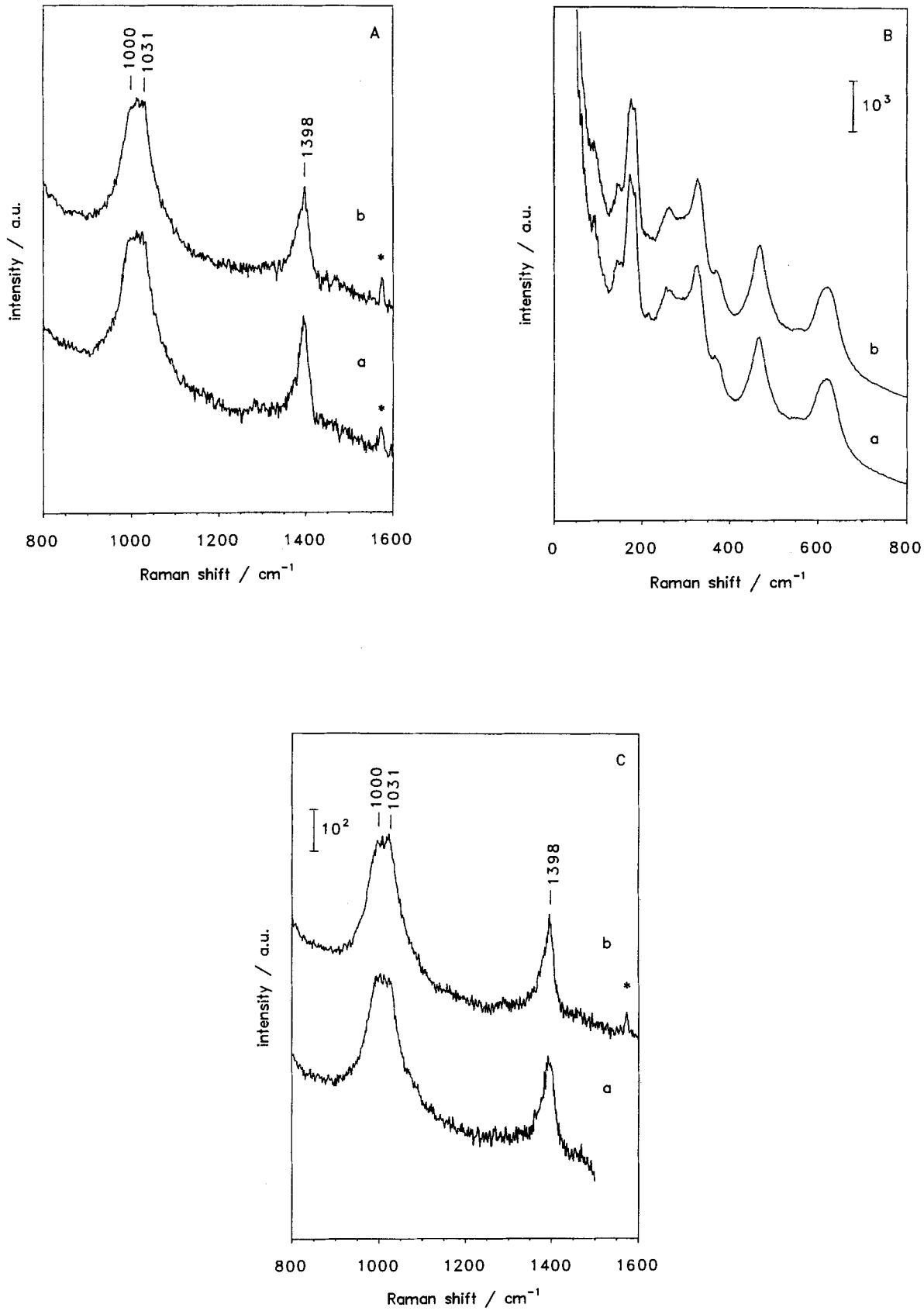

Fig. 4. In situ Raman spectra of sulfated zirconia recorded at 773 K (bands marked by asterisk (*) are plasma lines of the Ar^+ laser, used as a reference) (A) after reaction with He/*n*-butane, sulfate regime (a) activated fresh sample, (b) regenerated sample; (B) after reaction with H_2/*n*-butane, Zr–O regime (a) activated fresh sample, (b) regenerated sample; (C) after reaction with H_2/*n*-butane, sulfate regime (a) activated fresh sample, (b) regenerated sample.

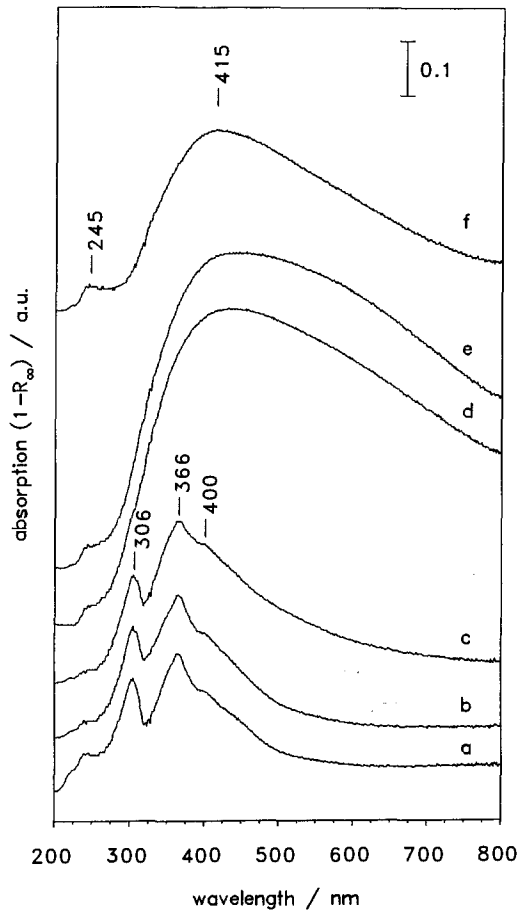

Fig. 5. UV-VIS-DR spectra (difference spectra) of sulfated zirconia (a) after reaction with He/*n*-butane at 473 K for 90 min; and after subsequent exposure to dry oxygen at increasing temperature for 30 min at (b) 293 K, (c) 423 K, (d) 523 K, (e) 623 K, (f) 723 K.

the absorption edge of the ZrO_2 by the principle adsorption of any organic or inorganic compounds at the surface and remains almost unchanged during the treatment in O_2 below 753 K.

In the following, experiments are described in which the deactivated ZrO_2/SO_4 catalyst was treated in O_2 at room temperature. These experiments are aimed at elucidating the chemistry occurring during oxidative regeneration processes.

Fig. 6A shows the UV-VIS-DR spectra after the reaction in He/*n*-butane at 473 K and a subsequent treatment in a flow of dry and wet O_2 at room temperature. Immediately after the contact with water, additional bands are observed at 430 (sh) and 454 nm (spectrum c in fig. 6A), which are strongly increasing with treatment time together with absorption bands at 393, 517 and 554 nm (spectra d–h in fig. 6A). The bands of allylic and polyenylic cations at 306 and 366 nm, respectively, seem to remain unchanged in this series (spectra a–f in fig. 6A). Consequently, they are not related to the bands at 430 and 455 nm. These absorption bands are attributed to quinone-type products, formed by oxidation of the aromatic compounds [25]. With further treatment in wet O_2 the two bands of allylic and polyenylic cations vanished. After 30 min (spectra g–k in fig. 6A) the absorption bands at 393, 430, 454, 517 and 554 nm start to decrease in intensity and a minor intense broad absorption band with maximum at 415 nm appears, which probably could be attributed to polycyclic aromatic compounds and condensed rings [23]. After subsequent treatment of the sample in a flow of dry oxygen at 753 K for 1 h, the spectrum of the fresh catalyst was again obtained.

The UV-VIS-DR spectrum a in fig. 6B was obtained for the catalyst after the reaction with H_2/*n*-butane at 473 K for 90 min. A very weak and broad absorption band at 410 nm could be attributed to polycyclic aromatic compounds and condensed rings, in agreement with the corresponding Raman spectra. The absence of bands for allylic or polyenylic cations is in agreement with the results of Chen et al. [22]. The treatment of the sample in dry O_2 at RT causes no changes in the spectrum (spectrum b in fig. 6B). After contact with wet O_2 additional bands at 430, 450, 521 and 542 nm appeared (spectra c–h in fig. 6B), as observed in the experiment with He as carrier gas. An additional weak absorption band at 341 nm did not seem to be correlated to the other bands. The origin of this band may be attributed to possible intermediates in the formation of quinone-type products. After 90 min in wet O_2 all the bands start to decrease in intensity with further treatment. An asymmetric broad band at 245 nm dominates the spectra for longer treatment periods. The lineshape and the intensity of this band is identical with the corresponding spectra of the experiments with He as the carrier gas (spectra f–k in figs. 6A and 6B); the band is consequently not related to the amount of adsorbed organic species.

3.4. Electron spin resonance (ESR)

The ESR spectrum of the activated sample (spectrum a in fig. 7A) shows a very weak signal with $g_\perp = 2.012$ and $g_\parallel = 2.004$. Torralvo et al. [26] reported a similar signal during the tetragonal to monoclinic phase transition of ZrO_2. They attributed this signal to paramagnetic oxygen defect centres in the bulk of ZrO_2. Iron impurities of the material caused a weak signal at $g = 4.25$, which is charateristic for Fe^{3+} in a tetrahedral and/or octahedral environment [27]. Additional weak signals at $g = 2.65$ (w) and 2.2 (br) originate from the cavity.

After exposure of the ZrO_2/SO_4 to He/*n*-butane at 473 K for 90 min additional signals at $g = 2.018$, 2.002 and 1.98 are found (spectrum b in fig. 7A). The intensity of the signal at $g = 1.98$ drastically increased by cooling from room temperature to 120 K, which is characteristic of transition metal ions. Morterra et al. [28] observed an axial spectrum with $g_\perp = 1.979$ and $g_\parallel = 1.951$ for ZrO_2 outgassed above 700 K, which they assigned to cus Zr^{3+} in octahedral symmetry with tetragonal distortion. Based on these results, the signal at 1.98 is attributed to cus Zr^{3+}, which is shifted and broadened by a strong dis-

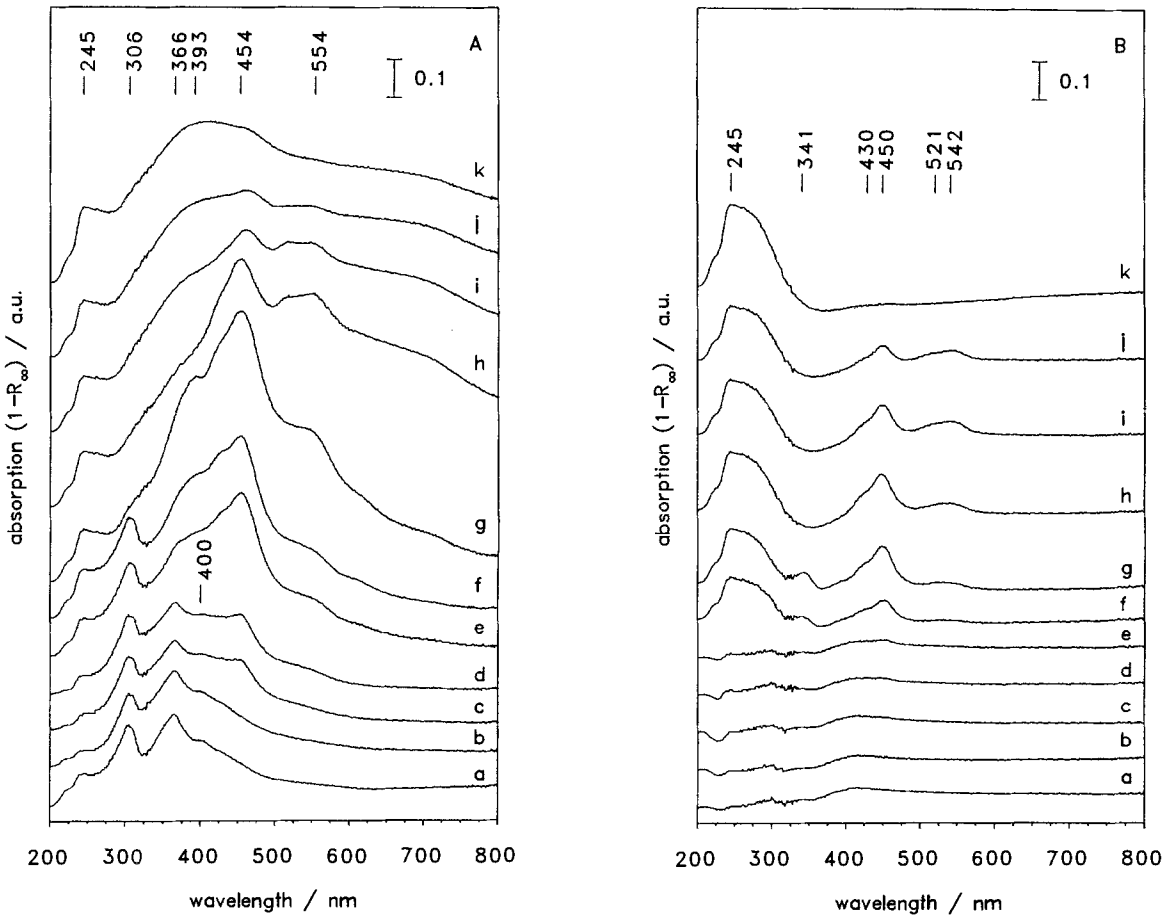

Fig. 6. UV-VIS-DR spectra (difference spectra) of sulfated zirconia (A) (a) after reaction with He/*n*-butane at 473 K for 90 min; (b) exposure to dry oxygen at 293 K for 1 h; and subsequent exposure to wet oxygen at 293 K for (c) 20 s, (d) 90 s, (e) 6 min, (f) 10 min, (g) 25 min, (h) 45 min, (i) 90 min, (j) 150 min, (k) 200 min; (B) (a) after reaction with H_2/*n*-butane at 473 K for 90 min; (b) exposure to dry oxygen at 293 K for 1 h; and subsequent exposure to wet oxygen at 293 K for (c) 20 s, (d) 6 min, (e) 10 min, (f) 25 min, (g) 45 min, (h) 90 min, (i) 150 min, (j) 200 min, (k) 15 h.

tortion of the symmetry and by other paramagnetic centers. The signal at $g = 2.002$ is attributed to organic radicals (see below), whereas the origin of the signal at $g = 2.018$ remains somewhat uncertain at present. Spectra recorded with increasing microwave power (10–200 mW) revealed an additional weak signal at $g = 2.04$, whose intensity seemed to be correlated to the signal at $g = 2.018$. Based on literature data [29], it is proposed that the signals are caused by some sulphur containing radicals, namely SO_4^-.

After exposure to dry oxygen at room temperature the signal at $g = 2.018$ vanishes or is superimposed by new signals at $g_1 = 2.027$ and $g_2 = 2.010$ (spectrum c in fig. 7A). These two signals increased at 423 K (spectrum d in fig. 7A) and could be assigned to adsorbed O_2^- together with a third signal at $g_3 = 2.003$ [30]. Chen et al. [22] observed a similar spectrum after the adsorption of benzene on ZrO_2/SO_4 and a subsequent treatment with dry oxygen. The authors proposed a reaction of Zr^{3+} with O_2 from the gas phase and the formation of adsorbed O_2^-. Jakob et al. [31] proved the presence of O_2^- on the surface of ZrO_2 after the reaction of O_2 with Zr–H groups, the latter being formed by preadsorption of H_2. As a consequence it is proposed, that the formation of O_2^- is caused by the presence of Zr–H groups, which are formed in the reaction with He/*n*-butane. This would be in agreement with the proposed mechanism of the formation of allylic and polyenylic cations. The thermal stability of O_2^- at 423 K is confirmed by results of Iwamoto and Lunsford [32], who found a very low reactivity of O_2^- on MgO in the presence of alkanes and alkenes. The signal at $g = 1.98$, assigned to cus Zr^{3+} decreases at higher temperatures, probably because of the reaction with O_2.

As the temperature is increased to 523 and 623 K, the intensity of the O_2^- signal decreases (spectra e and f in fig. 7B). Simultaneously the signal intensity at $g = 2.002$ is drastically increased by the formation of polycyclic aromatic and condensed rings in agreement with the changes observed in the UV-VIS-DR spectra (spectra d and e in fig. 5). The hyperfine splitting remains unresolved, this being a typical effect in the carbonization of organic compounds [33]. The signal decreases after treatment at 723 K by the oxidation of the organic deposits (spectrum g in fig. 7B). A weak signal at $g = 1.975$ may be attributed to Zr^{3+}. The decrease of the

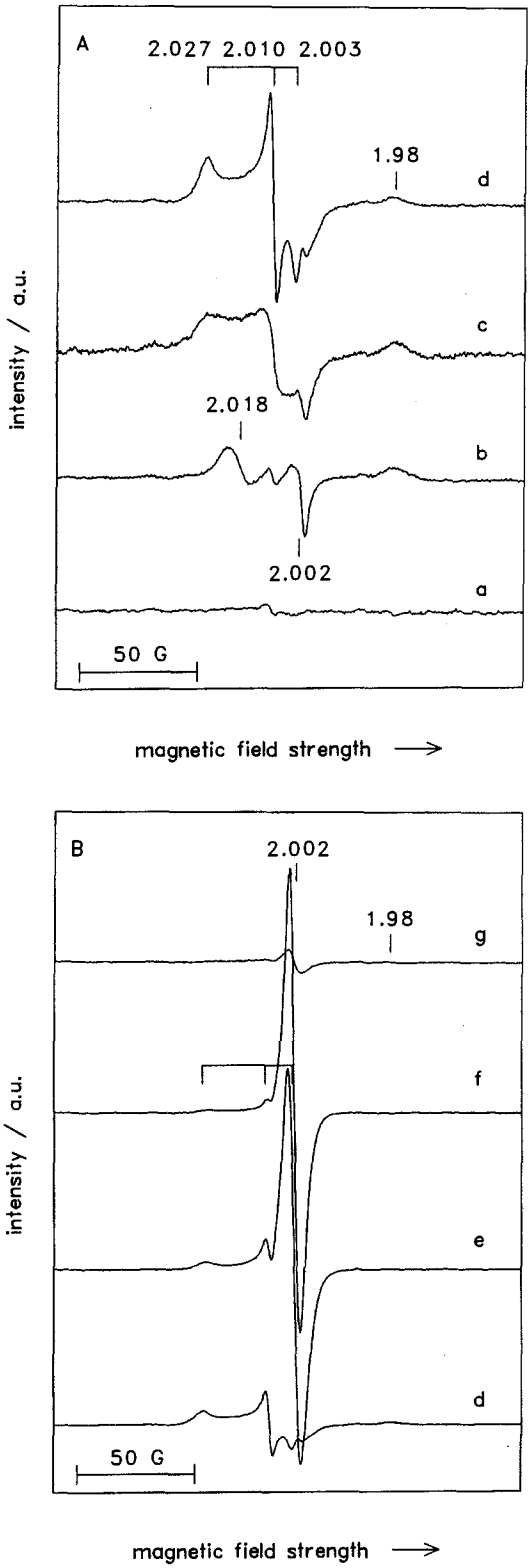

Fig. 7. ESR spectra of sulfated zirconia (A) (a) activated sample; (b) after reaction with He/*n*-butane at 473 K for 90 min; and after subsequent exposure to dry oxygen with increasing temperature for 30 min at (c) 293 K, (d) 423 K; and (B) (d) 423 K (same as spectrum d in fig. 7A), (e) 523 K, (f) 623 K, (g) 723 K.

linewidth of this signal, as compared to the other spectra, suggests that adsorbed products, which caused a broadening of the signal, were removed by the treatment in O_2.

Fig. 8A shows the ESR spectra of the ZrO_2/SO_4 catalyst after exposure in He/*n*-butane at 473 K for 90 min and a subsequent treatment in wet O_2. After 6 min in wet O_2 weak signals are observed at $g = 2.010$, 2.002 and 1.98 (spectrum d in fig. 8A). The signals of O_2^- disappeared, probably by reaction with water: $2O_2^- + 2H_2O \rightarrow O_2 + H_2O_2 + 2OH^-$. The formation of H_2O_2 is in agreement with the observation of quinone-type products in the UV-VIS-DR spectra (fig. 6A). In a similar way SO_4^- reacts with water: $2SO_4^- + H_2O \rightarrow 2HSO_4^- + \frac{1}{2}O_2$, which results in the disappearance of the signal at $g = 2.018$. After 90 min only a single broad signal at $g = 2.002$ could be identified (spectrum e in fig. 8A). Subsequently the sample was calcined in a flow of dry O_2 at 723 K for 4 h. UV-VIS-DR spectra (not shown) indicated a slightly enhanced absorption within the entire recorded spectral range. The ESR spectrum f in fig. 8A shows weak signals at $g = 2.010$ and 1.979, which are attributed to paramagnetic oxygen centers [26] and cus Zr^{3+}, respectively. A broad signal near the free electron is probably caused by some organic residues.

The ESR spectrum of the sample after exposure to H_2/*n*-butane (spectrum b in fig. 8B) is quite similar to that obtained in the He/*n*-butane experiment (spectra b in figs. 7A and 8A). The treatment in dry oxygen at room temperature produces a well resolved spectrum with known signals of O_2^- (spectrum c in fig. 8B). In the presence of H_2, the formation of the Zr–H groups typically occurs by the dissociative adsorption of H_2 on ZrO_2 [34]. Spectrum d in fig. 8B was recorded 6 min after exposure in wet O_2. It shows only broadening of the signals. Signals of adsorbed O_2^- and SO_4^- are still present, in contrast to the corresponding ESR spectrum of the He experiment. Further treatment with wet O_2 reduces the intensity of all signals except that of the organic contaminants with $g = 2.002$ (spectra e–f in fig. 8B). After the calcination in a flow of dry oxygen at 723 K, the signal at 2.003 disappeared and a signal of Zr^{3+} at $g = 1.979$ is identified.

4. Conclusions

Deactivation of the ZrO_2/SO_4 catalyst during the isomerization of *n*-butane to isobutane in the absence of H_2 is presumably caused by the formation of allylic and polyenylic cations and polycyclic aromatic compounds, which could be observed by in situ Raman and UV-VIS-DR spectroscopy. The former products are known to be intermediates in the formation of higher unsaturated hydrocarbons and aromatic compounds [35]. Allylic and polyenylic cations can be produced from alkenes in the presence of Lewis acid sites, namely cus Zr^{4+}, by hydride abstraction and formation of Zr–H groups [4]. Adsorbed O_2 from the gas phase is proposed to react with Zr–H to

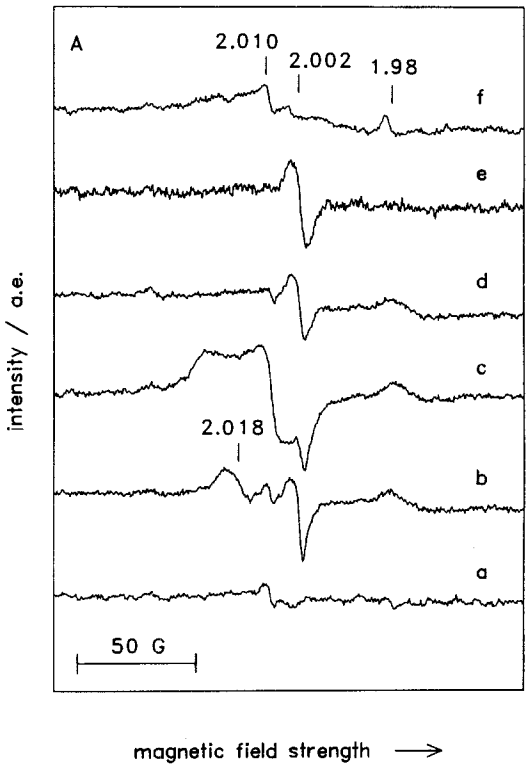

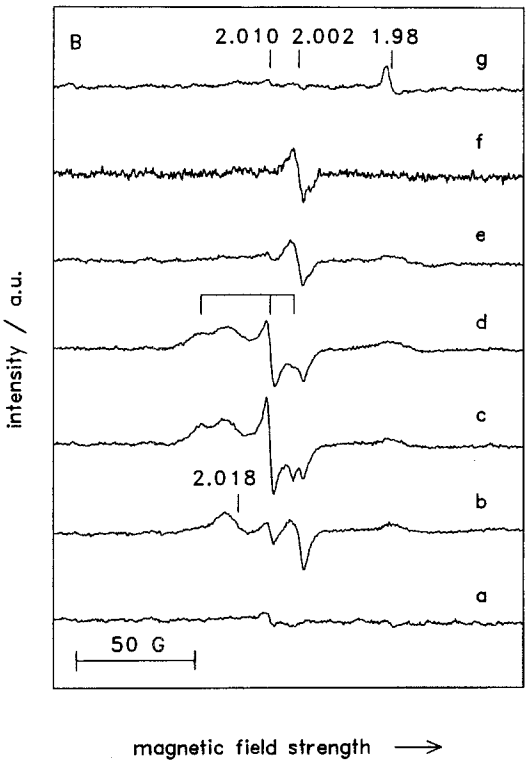

Fig. 8. ESR spectra of sulfated zirconia (A) (a) activated sample, (b) after reaction with He/*n*-butane at 473 K for 90 min; (c) exposure to dry oxygen at 293 K for 1 h; and subsequent exposure to wet oxygen at 293 K for (d) 6 min, (e) 90 min, (f) calcination in a flow of dry oxygen at 723 K for 4 h; (B) (a) activated sample, (b) after reaction with H_2/*n*-butane at 473 K for 90 min; (c) exposure to dry oxygen at 293 K for 1 h; and subsequent exposure to wet oxygen at 293 K for (d) 6 min, (e) 25 min, (f) 18 h, (g) calcination in a flow of dry oxygen at 723 K for 4 h.

form O_2^- which was observed by ESR. UV-VIS-DR spectroscopy showed, that the allylic and polyenylic cations are stabilized by the surface of the catalyst in the presence of O_2 up to 423 K.

Addition of H_2 to the reaction mixture results in a complete suppression of the formation of the allylic and polyenylic cations. Instead, Zr–H groups are created, which is confirmed by the formation of O_2^-. This suggests that H_2 is inhibiting the formation of allylic and polyenylic cations by occupation of cus Zr^{4+}. Small amounts of aromatic compounds, presumably formed via other intermediates, suggest that H_2 also decreases the coke formation by the inhibition of the dehydrogenation step.

The results of this study emphasize the advantageous effect of H_2 in that it strongly reduces the catalyst deactivation. The results also demonstrate that oxidative regeneration of ZrO_2/SO_4 is possible in which process the original nature of the catalyst and its initial catalytic activity for *n*-butane isomerization are completely restored. This bears some potential for the design of technologies (e.g. similar to FCC) for *n*-butane isomerization that might be economically feasible.

Acknowledgement

This work was financially supported by the Deutsche Forschungsgemeinschaft (SFB 338), the Bayerischer Forschungsverbund Katalyse FORKAT, and the Fond der Chemischen Industrie. The authors thank Professor M. Che and Dr. Z. Sojka for valuable discussions.

References

[1] H. Hino and K. Arata, J. Chem. Soc. Chem. Commun. (1980) 851.
[2] K. Tanabe, M. Itoh, K. Morishige and H. Hattori, in: *Preparation of Catalysts*, eds. B. Delmon, P.A. Jacobs and G. Poncelet (Elsevier, Amsterdam, 1976) p. 65.
[3] H. Hino and K. Arata, J. Chem. Soc. Chem. Commun. (1979) 1148.
[4] C.-Y. Hsu, C.R. Heimbuch, C.T. Armes and B.C. Gates, J. Chem. Soc. Chem. Commun. (1992) 1645.
[5] A. Jatia, C. Chang, J.D. MacLeod, T. Okubo and M.E. Davis, Catal. Lett. 25 (1994) 21.
[6] G.A. Olah, G.K.S. Prakash and J. Sommer, *Superacids* (Wiley-Interscience, New York, 1985), and references therein.
[7] C. Guo, S. Lieo, Z. Qian and K. Tanabe, Appl. Catal. 107 (1994) 239.
[8] C. Guo, S. Yao, J. Cao and Z. Qian, Appl. Catal. 107 (1994) 229.
[9] F. Garin, D. Andriamasinoro, A. Abdulsamad and J. Sommer, J. Catal. 131 (1991) 199.
[10] V. Adeeva, J.W. de Haan, J. Jänchen, G.D. Lei, V. Schünemann, L.J.M. van de Ven, W.M.H. Sachtler and R.A. van Santen, J. Catal. 151 (1995) 364.
[11] V. Adeeva, G.D. Lei and W.M.H. Sachtler, Appl. Catal. A 118 (1994) L11
[12] K. Ebitani, J. Konishi and H. Hattori, J. Catal. 130 (1991) 257.

[13] B.H. Davis, R.A. Keogh and R. Srinivasan, Catal. Today 20 (1994) 219.
[14] H. Zeilinger, Doctoral Thesis, Universität München, Germany (1991).
[15] P. Knoll, R. Singer and W. Kiefer, Appl. Spectrosc. 44 (1990) 776;
Spielbauer, Appl. Spectrosc., accepted.
[16] E. Bosch, Diploma Thesis, Universität München, Germany (1994).
[17] T. Riemer, D. Spielbauer, M. Hunger, G.A.H. Mekhemer and H. Knözinger, J. Chem. Soc. Chem. Commun. (1994) 1181.
[18] N.B. Colthup, L.H. Daly and S.E. Wiberley, *Introduction to Infrared and Raman Spectroscopy,* 3rd Ed. (Academic Press, New York, 1990).
[19] J.-P. Lange, A. Gutsze, J. Allgeier and H.G. Karge, Appl. Catal. 45 (1988) 345.
[20] P. E. Eberly Jr., J. Phys. Chem. 71 (1967) 1717.
[21] M. Bensitel, O. Saur, J.C. Lavalley and B.A. Morrow, Mater. Chem. Phys. 19 (1988) 147.
[22] F.R. Chen, G. Coudurier, J.-F. Joly and J.C. Vedrine, J. Catal. 143 (1993) 616.
[23] H.G. Karge, M. Laniecki, M. Ziolek, G. Onyestyak, A. Kiss, P. Kleinschmitt and M. Siray, in: *Zeolites: Facts, Figures, Future*, eds. P.A. Jacobs and R. van Santen (Elsevier, Amsterdam, 1989) p. 1327.
[24] T.S. Sorensen, J. Am. Chem. Soc. 87 (1965) 5075.
[25] M. Hesse, H. Meier and B. Zeeh, *Spektrokopische Methoden in der organischen Chemie*, 3rd Ed. (Thieme, Stuttgart, 1987) p. 18.
[26] M.J. Torralvo, M.A. Alario and J. Soria, J. Catal. 84 (1984) 473.
[27] T. Castner Jr., G.S. Newell, W.C. Holton and C.P. Slichter, J. Chem. Phys. 32 (1960) 668.
[28] C. Morterra, E. Giamello, L. Orio and M. Volante, J. Phys. Chem. 94 (1990) 3111.
[29] J.R. Morton, D.M. Bishop and M. Randic, J. Chem. Phys. 45 (1966) 1885.
[30] M. Che and A.J. Tench, Adv. Catal. 32 (1983) 1;
M. Setaka and T. Kwan, Bull. Chem. Soc. Jpn. 43 (1970) 2727.
[31] K.-H. Jacob, E. Knözinger and S. Benfer, J. Chem. Soc. Faraday Trans. 90 (1994) 2969.
[32] M. Iwamoto and J.H. Lunsford, J. Phys. Chem. 84 (1980) 3079.
[33] A. Gutsze and S. Orzeszko, Adv. Colloid Interf. Sci. 23 (1985) 215.
[34] J. Kondo, Y. Sakata, K. Domen, K. Maruya and T. Onishi, J. Chem. Soc. Faraday Trans. 86 (1990) 397.
[35] H.G. Karge, in: *Introduction to Zeolite Science and Practice*, eds. H. van Bekkum, E.M. Flanigen and J.C. Jansen (Elsevier, Amsterdam, 1991) p. 531.